Carbon nanofiber supercapacitors with large areal capacitances

James R. McDonough, Jang Wook Choi, Yuan Yang, Fabio La Mantia, Yuegang Zhang, and Yi Cui

---

Articles you may be interested in

Electrochemical properties of carbon nanofiber web as an electrode for supercapacitor prepared by electrospinning
Applied Physics Letters **83**, 1216 (2003); 10.1063/1.1599963

Supercapacitors specialities - Materials review
AIP Conference Proceedings **1597**, 98 (2014); 10.1063/1.4878482

High power electrochemical capacitors based on carbon nanotube electrodes
Applied Physics Letters **70**, 1480 (1997); 10.1063/1.118568

Printed energy storage devices by integration of electrodes and separators into single sheets of paper
Applied Physics Letters **96**, 183502 (2010); 10.1063/1.3425767

Supercapacitors using singlewalled carbon nanotube electrodes
AIP Conference Proceedings **590**, 241 (2001); 10.1063/1.1420099

Flexible solid-state paper based carbon nanotube supercapacitor
Applied Physics Letters **100**, 104103 (2012); 10.1063/1.3691948

Carbon nanofiber supercapacitors with large areal capacitances

James R. McDonough,[1] Jang Wook Choi,[1] Yuan Yang,[1] Fabio La Mantia,[1] Yuegang Zhang,[2,a)] and Yi Cui[1,a)]

[1]*Department of Materials Science and Engineering, Stanford University, Stanford, California 94305, USA*
[2]*Lawrence Berkeley National Laboratory, Berkeley, California 94720, USA*

We develop supercapacitor (SC) devices with large per-area capacitances by utilizing three-dimensional (3D) porous substrates. Carbon nanofibers (CNFs) functioning as active SC electrodes are grown on 3D nickel foam. The 3D porous substrates facilitate a mass loading of active electrodes and per-area capacitance as large as 60 mg/cm^2 and 1.2 F/cm^2, respectively. We optimize SC performance by developing an annealing-free CNF growth process that minimizes undesirable nickel carbide formation. Superior per-area capacitances described here suggest that 3D porous substrates are useful in various energy storage devices in which per-area performance is critical. © 2009 American Institute of Physics. [doi:10.1063/1.3273864]

Supercapacitors (SCs) are useful in various applications such as in hybrid energy systems in vehicles, digital telecommunication systems, uninterrupted power supply for computers, and pulsed laser techniques, due to their high power densities (>10 kW/kg), long cycle lives ($>10^6$ cycles), and safe operation. In order to improve the performance of carbon-based SCs, carbon nanofibers (CNFs) and carbon nanotubes (CNTs) have been studied immensely in recent years due to their efficient ion diffusion pathways.[1–6] Although some of these CNF SCs achieve relatively high specific capacitances of >100 F/g, the mass loading is often very low, resulting in a capacitance per area in the mF/cm^2 range. For applications such as small scale electronics or stationary energy storage devices, the amount of energy stored per area is more important than energy per mass.

In this study, we use three-dimensional (3D) porous metallic foam substrates to address the areal energy storage problems of current SC devices. Active CNF materials can be loaded onto, or grown from, the highly conductive 3D metallic backbone, allowing for a higher mass loading of active materials per area than a simple two-dimensional (2D) flat substrate would. In our case, CNFs with diameters ranging from 10–100 nm are directly grown on 3D Ni foam. TEM images of fibers indicate that our thermal CVD growth results only in CNF growth rather than CNT growth (see supplementary information Fig. S1).[10] Carbon aerogels (CAs) have also attracted interest as highly porous 3D SC electrodes. Lv *et al.* recently fabricated CA electrodes with nanosized MnO_2 loaded inside aerogel pores.[7]

Preparation of our CNF-based SC electrodes consists of two steps. First, a piece of Ni foam (Ni foam 95% porosity, 500 g/m^2 surface area, MarkeTech International) approximately $1 \times 1 \times 0.2$ cm^3 is conformally coated with a 1 nm alumina layer by atomic layer deposition (ALD, Cambridge NanoTech Inc.). The alumina layer passivation serves two purposes. First, the buffering alumina layer protects the Ni foam backbone from being transformed to undesirable Ni_3C by inhibiting the diffusion of the carbon precursor into the Ni. Second, the alumina layer circumvents oxidation-

reduction steps normally required for CNF growth processes. Planar Ni catalysts prefer planar carbon layer growth instead of CNFs due to a lack of nonplanar nucleation sites during a chemical vapor deposition (CVD) process. Therefore, in most thermal CVD CNF growth processes, an annealing step is normally needed to roughen the planar Ni surface and to prevent planar carbon layer formation. Because this annealing step is done in air, a subsequent reduction step in H_2 is required to reduce the nickel oxide back to metallic Ni. With the thin alumina layer, however, the growth process can be simplified to a single annealing-free step because the porous alumina layer helps the nucleation and growth of CNFs and prevents planar carbon growth. The growth process is performed by flowing 50 sccm H_2, 25 sccm C_2H_4, and 75 sccm Ar over the alumina-coated Ni foam substrates at 470 °C inside a tube furnace for 30 min. Figure 1(a) provides a photograph comparing Ni foam before and after CNF growth. The originally silver colored Ni foam changes to a uniform black color with the backbone and large voids in the foam still visible. This observation suggests a uniform CNF coating on the Ni foam, as confirmed by the SEM images before [Fig. 1(b)] and after [Figs. 1(c) and 1(d)] CNF growth. Uniform CNF coverage enables the entire 3D structure of the Ni foam after CNF growth to contribute to supercapacitor performance. The electrolyte solution can easily penetrate the large voids in the Ni foam and contribute to the
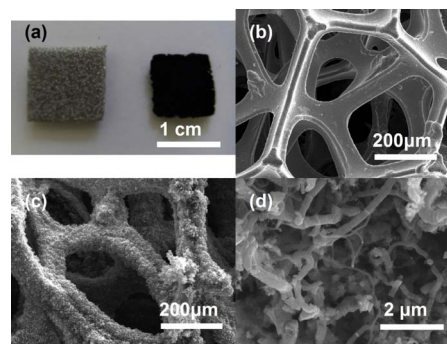

FIG. 1. (Color online) (a) Photograph of Ni foam before and after CNF growth. (b) SEM image of pristine Ni foam. SEM images of CNFs after growth at (c) low and (d) high magnification confirm that a conformal layer of CNFs coats the Ni foam.

a)Authors to whom correspondence should be addressed. Electronic addresses: yzhang5@lbl.gov and yicui@stanford.edu.
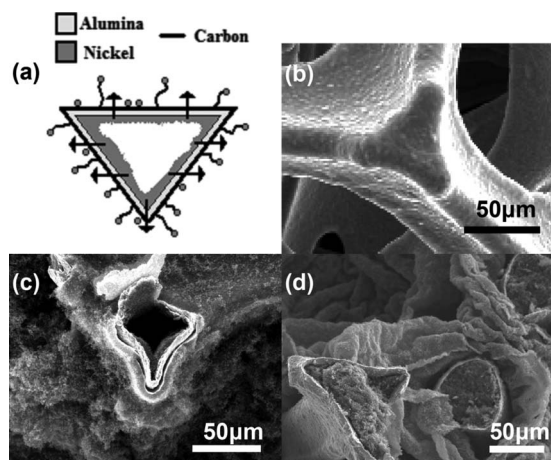
FIG. 2. (a) Proposed mechanism for Ni diffusion during CNF growth. (b) SEM image of pristine Ni foam, indicating a solid cross section. (c) SEM image of alumina-coated Ni foam after CNF growth, indicating a hollow cross section. (d) SEM image of noncoated Ni foam after CNF growth, indicating a solid Ni_3C cross section.

double-layer capacitance on the CNF surface throughout the entire 3D Ni foam network.

Three synergistic aspects of this synthesis procedure are noteworthy: First, the alumina coating on the Ni foam during the CNF growth process minimizes the formation of Ni_3C, a highly brittle material, within the Ni foam backbone. The minimized Ni_3C formation is likely due to the alumina layer functioning as a buffer layer. During the growth process at 470 °C the alumina layer controls the ethylene decomposition and inward carbon diffusion. Still, Ni diffuses out through the alumina layer, forming catalytic Ni particulates, and thus works as a catalyst for the CNF growth [Fig. 2(a)]. We believe that Ni can diffuse outward through the alumina layer due to small cracks or pores formed in the alumina layer during heating. This idea becomes more obvious from a direct comparison with the noncoated samples. While the originally solid Ni backbone [Fig. 2(b)] becomes hollow [Fig. 2(c)] for the alumina-coated samples, as a result of the controlled outward Ni diffusion through the alumina buffer layer, the nickel backbone remains solid and transforms to Ni_3C for noncoated samples [Fig. 2(d)] upon direct exposure to ethylene gas. In fact, we observed a mass increase of 60 mg/cm^2 during CNF growth for our alumina-coated Ni foam samples but a 108 mg/cm^2 increase for samples without alumina. The prevention of Ni_3C formation is responsible for the nearly 50% mass difference during growth of coated versus noncoated samples. This difference is also reflected in the disparate mechanical properties of the two samples. The alumina-coated samples, with minimal Ni_3C, are far less brittle than the Ni_3C-rich noncoated samples. Thus, the alumina coating helps protect the Ni foam backbone from being converted to Ni_3C. Second, the passivation with the alumina layer and H_2 flow during growth make a normally required annealing step unnecessary. For CNF growth, Ni particulates must be formed to act as catalytic nucleation and growth sites.[8] These particulates are normally formed by exposing a planar Ni catalyst to a high temperature annealing step in air followed by a subsequent H_2 reduction step to reform metallic Ni from nickel oxide. The result of the oxidation-reduction process is a roughened Ni surface which inhibits parasitic planar carbon formation during CNF
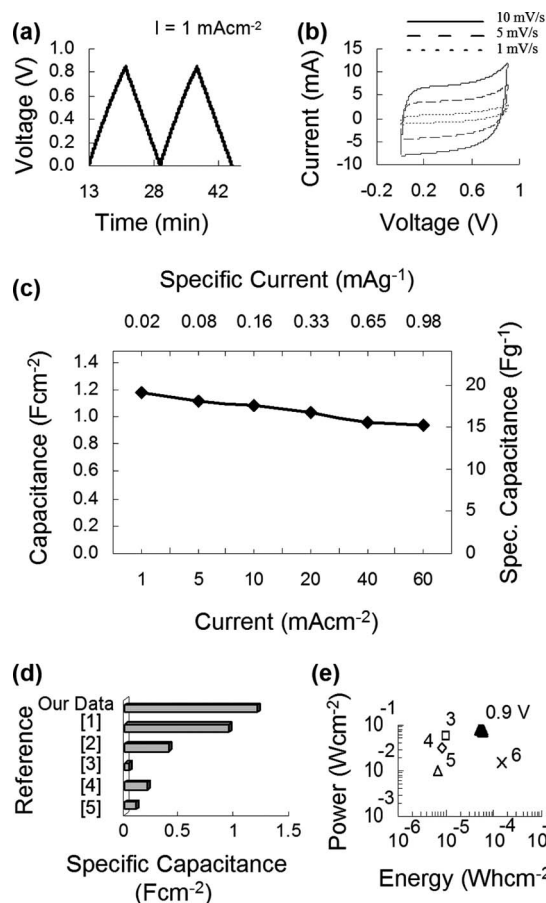

FIG. 3. (a) Voltage profile at 1 mA/cm^2 (dc current, zero frequency). (b) Cyclic voltammograms for our samples, exhibiting rectangular behavior. (c) Plot of specific capacitance vs specific current, both per-mass and per-area. (d) Bar graph comparing our per-area capacitance to those previously reported. (e) Per-area Ragone plot comparing our per-area power and energy densities to those previously reported.

growth. But, in our case, the entire process consists of only a single growth step. We believe that H_2 gas flow during CNF growth enables direct exposure and reduction of the native oxide layer on the Ni foam to H_2 via cracks and pores through the alumina film. Finally, the temperature required for the overall process is lower than those for normal CNF and CNT thermal chemical vapor deposition (CVD) growth processes. CVD methods for CNF and CNT growth alike with nonalloy catalysts generally require higher temperatures (545–1000 °C).[9] Consequently, the alumina passivation not only circumvents the annealing step but also lowers the overall process temperature significantly.

The SC cells in our study were comprised of symmetric CNF/Ni foam electrodes and a filter paper separator immersed in a 2 M Li_2SO_4 aqueous electrolyte solution. Detailed cell preparation procedures can be found in the supplementary information.[10] Figures 3(a) shows a voltage profile for our device under a 1 mA/cm^2 current density. The internal cell resistance calculated by the IR voltage drop in the curve was found to be 2.5 Ω. This internal resistance value was consistent with the internal resistance calculated by electrochemical impedance spectroscopy (supplementary information [Fig. S2]) (Ref. 10) which also indicated a resistance of 1.5 Ω inside the pores between adjacent CNFs. The ideal triangular shape of the charging and discharging curves provides compelling evidence that capacity is due only to

double-layer charging and not side reactions. Further evidence for the absence of side reactions in our devices is provided by cyclic voltammograms which approach ideal rectangular behavior with no redox peaks [Fig. 3(b)]. Figure 3(c) illustrates that our supercapacitor performance does not degrade to a large degree in higher power operations, due to highly efficient ion diffusion pathways. Note that while the specific currents in Fig. 3(c) are low due to the high CNF mass loading in the devices, the nominal current densities are high (1 to 60 mA/cm^2). Figure 3(d) demonstrates that our capacitance per area of 1.2 F/cm^2, as a result of our high device mass loading, is greater than previously reported results for CNF- and CNT-based supercapacitors.[1–5] Finally, Fig. 3(e) provides a comparison of our per-area CNF supercapacitor power and energy densities to previously reported results.[3–6] By utilizing the entire 3D Ni foam structure, our mass loading of ~60 mg/cm^2 CNFs enables superior per-area performance results. Furthermore, device stability was confirmed by charging/discharging cells over 3,000 cycles with an average Coulombic efficiency of 99.82%. Cycling data are presented in the supplementary information [Fig. S2].[10]

In conclusion, we have demonstrated supercapacitors with very high active material mass loadings and thus superior per-area capacitances, energy densities, and power densities. These are obtained by utilizing the entire surface area of CNFs on 3D metallic foam structures. Using an improved low-temperature thermal CVD CNF growth process, made possible by a thin alumina coating on pristine Ni foam, we are able to minimize Ni$_3$C formation within the Ni foam backbone which not only deteriorates the SC performance but also increases the brittleness of the SC electrodes. We expect our approaches can be used to improve the performance of various energy storage devices.

[1]K. An, W. Kim, Y. Park, J. Moon, D. Bae, S. Lim, Y. Lee, and Y. Lee, Adv. Funct. Mater. **11**, 387 (2001).
[2]D. N. Futaba, K. Hada, T. Yamada, T. Hiraoka, Y. Hayamizu, Y. Kakudate, O. Tanake, H. Hatori, M. Yumura, and S. Iijima, Nature Mater. **5**, 987 (2006).
[3]C. Du, J. Yeh, and N. Pan, Nanotechnology **16**, 350 (2005).
[4]C. Niu, E. K. Sichel, R. Hoch, D. Moy, and H. Tennent, Appl. Phys. Lett. **70**, 1480 (1997).
[5]C. Huang, Y. Wu, C. Hu, and Y. Li, J. Power Sources **172**, 460 (2007).
[6]F. Pico, J. M. Rojo, M. L. Sanjuan, A. Anson, A. M. Benito, M. A. Callejas, W. K. Maser, and M. T. Martinez, J. Electrochem. Soc. **151**, A831 (2004).
[7]G. Lv, D. Wu, and R. Fu, J. Non-Cryst. Solids **355**, 2461 (2009).
[8]J. K. Chinthaginjala, D. B. Thakur, K. Seshan, and L. Lefferts, Carbon **46**, 1638 (2008).
[9]H. Dai, *Carbon nanotubes: Synthesis, Structure, Properties and Application* (Springer, New York, 2001), pp. 29–54.
[10]See EPAPS supplementary material at http://dx.doi.org/10.1063/1.3273864 for supercapacitor cell preparation and data analysis, supercapacitor impedance data and capacity retention, and TEM characterization of carbon nanofibers..